The Structure of Alkali Metal Derivatives of Azoles: N−σ versus π Structures

Fernando Blanco, Ibon Alkorta,* and Jose Elguero

Instituto de Química Médica (CSIC), Juan de la Cierva, 3, 28006-Madrid, Spain

Received: March 5, 2008; Revised Manuscript Received: May 26, 2008

High level *ab initio* calculations have been used to study the relative stability of N−σ and π configurations of the neutral alkaline derivatives of azoles. The N−σ structure is the one normally expected for nonionized azolate salts. However, the results show that in the case of the pyrrole and imidazole the π configuration is more stable than the N−σ one. The preference of the N−σ vs π configurations is related to the presence or the absence of two contiguous nitrogen atoms in the azole ring. A search in the CSD shows that some pyrrolate and imidazolate salts exist in solid phase in the π configuration.

Introduction

The knowledge of the structures formed by cations with heterocycles in their neutral or anionic forms is of great importance to understand a number of biochemical mechanisms, recognition processes in supramolecular chemistry[1,2] and the physicochemical properties of ionic liquids.[3] The most common azoles (nitrogenated five membered heterocycles) in biomolecules are pyrrole (tryptophan, serotonin, porphyrins) and imidazole (histidine, histamine, B12 vitamin). Neutral salts of azoles are known formally to be in three possible combinations: azolium/anion, azolate/cation and azolium/azolate, the first one being the most common.[4,5] In the absence of polar environments, the two formal ionic fragments are linked, in many cases, by partial covalent bonds similar to the one described for the isolated benzyllithium.[6]

Recent experimental and theoretical studies on alkaline (Li, Na and K) derivatives of pyrazoles[7–9] have shown the presence of two minima, one with the metal linked to the nitrogen atoms and another above the ring. In those derivatives, the former minima were between 39.7 and 15.9 kJ mol^{-1} more stable than the latter, at the MP2/VDZ computational level, the difference being larger for the derivatives of the smaller metal atoms. In another experimental study, alkaline salts of pyrrolates complexed with crown ethers show the metal linked to the nitrogen atom for the smaller metallic atoms and above the heterocyclic ring in the larger ones.[10] The theoretical study of the M-N_5 system, where M corresponds to the alkaline atoms, has indicated two minima with C_{2v} and C_{5v} symmetry.[11]

In the present article, we report a study of the geometries, energies and electronic properties of the N−σ and π structures of the neutral alkaline derivatives of all azoles (Scheme 1) using DFT and *ab initio* methods.

Methods. Initially, the geometries of the systems included in this study have been fully optimized with the hybrid HF/DFT B3LYP method[12,13] and the 6-31+G(d,p) basis set[14] with the Gaussian-03 program.[15] These optimized geometries have been used as starting point in the composite G2 calculations.[16] In all cases, frequency calculations confirmed that the geometries obtained correspond to energetic minima. For some selected cases, optimization at the MP2/aug-cc-pVTZ calculation has been carried out.[17,18] The values of the free energy calculations correspond to 298.15 K and 1 atm of pressure. All the analysis of the electronic properties of these systems has been performed using the B3LYP/6-31+G(d,p) wave function.

SCHEME 1: N−σ and π Structures of the Alkaline Metal Derivatives of the Azoles

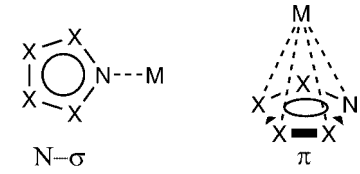

X = N or CH, M = Li, Na, K

The electron density of the molecules has been analyzed within the atoms in molecules (AIM) methodology[19] with the AIMPAC,[20] MORPHY98,[21] and AIM2000 packages.[22] The atomic properties (volume, charge and energy) have been evaluated by integration of the electron density within the atomic basins. The integrated Laplacian has been taken as an initial measure of the quality of the integration. Ideally, the Laplacian as integrated over any atomic basins of a system should result in a null value; however, values smaller than 1×10^{-3} have been shown to provide only negligible errors in energy and charge results.[23] Thus, the conditions of the integration have been adjusted when this requirement was not satisfied. In the molecules studied here, the largest absolute value of the error in the energy and charge has been 1.5 kJ mol^{-1} and 0.002 e.

A natural bond orbital analysis,[24] using the NBO program,[25,26] has been used to study orbital-based donor−acceptor interactions and their influence upon geometrical parameters. The electrostatic potential generated by the molecule upon its surroundings has been calculated using facilities within the Gaussian-03 package, and the minimum in this potential has also been localized and energetically evaluated. Such minima in the molecular electrostatic potential (MEP) have been widely used to analyze *a priori* the reactivity and complex formation of molecules.[27–32]

Two separate indexes of aromaticity have been investigated, employing both geometric (harmonic oscillator model of aromaticity, HOMA) and magnetic criteria (nuclear independent chemical shift, NICS). The geometry-based HOMA index[33] can be evaluated from the aromatic bond lengths by means of the equation HOMA $= 1 - [(\alpha/n)\sum(R_{opt} - R_i)^2]$, where R_{opt} and R_i

* Author to whom correspondence should be addressed. Fax: (+34) 91 564 48 53. E-mail: ibon@iqm.csic.es. Homepage: http://www.iqm.csic.es/are.

10.1021/jp801936v CCC: $40.75
Published on Web 07/31/2008

TABLE 1: ΔΔ*G*° (kJ mol^{-1}) of the Minima Obtained at the B3LYP/6-31+G(d,p) and G2 Computational Levels[a]

azole	alkaline confign	B3LYP/6-31+G(d,p)			G2		
		Li	Na	K	Li	Na	K
pyrrole	N−σ	36.4 (48.8)	17.7 (29.0)	23.3	40.0	26.9	44.6
pyrrole	π	**0.0 (0.0)**	**0.0 (0.0)**	**0.0**	**0.0**	**0.0**	**0.0**
pyrazole	N−σ	0.0	0.0	0.0	0.0	0.0	0.0
pyrazole	π	47.0	*b*	*b*	40.0	*b*	*b*
imidazole	N−σ	20.9 (36.59)	9.7 (24.26)	17.4	26.9	14.3	34.9
imidazole	π	**0.0 (0.0)**	**0.0 (0.0)**	**0.0**	**0.0**	**0.0**	**0.0**
1,2,3-triazole	N1−σ	0.0	0.0	0.0	0.0	0.0	0.0
1,2,3-triazole	π	46.1	31.6	21.2	37.1	26.4	11.6
1,2,4-triazole	N1−σ	0.0	0.0	0.0	0.0	0.0	0.0
1,2,4-triazole	N4−σ	78.1	66.4	63.4	77.7	63.8	65.4
1,2,4-triazole	π	56.5	*b*	*b*	49.4	*b*	*b*
tetrazole	N1−σ	0.0	1.6	1.9	0.0	0.1	1.0
tetrazole	N2−σ	0.2	0.0	0.0	1.6	0.0	0.0
tetrazole	π	56.5	*b*	*b*	37.1	*b*	*b*
pentazole	N−σ	0.0	0.0	0.0	0.0	0.0	0.0
pentazole	π	45.2	29.5	13.2	30.7	18.8	0.5

[a] In parentheses are shown the MP2/aug-cc-pVTZ// MP2/aug-cc-pVTZ relative energies. [b] These configurations spontaneously revert to the more stable N−σ ones.

correspond to optimal bond lengths and bond lengths in the real system, respectively. The variable α is an empirical factor chosen to provide a HOMA value of zero for the Kekulé structure of the archetypal aromatic system and a value of one for the hypothetical system with all bond lengths equal to the optimal value R_{opt}. Finally, n is the number of the bonds considered in the system. The values used here for R_{opt} are 1.388, 1.334 and 1.309 Å with α equal to 257.7, 93.52 and 130.33 for the C−C, C−N and N−N bonds, respectively.[33] The second aromaticity index, the NICS, is defined as the negative absolute magnetic shielding computed in the center of the aromatic ring.[34] Also presented here is the NICS(1) index calculated at 1 Å above the ring center.[35] Rings with highly negative NICS values are said to be aromatic whereas those with positive values are described as antiaromatic.

In addition, the natural resonance theory (NRT)[36–38] has been applied to evaluate the contribution of each Lewis structure to the *ab initio* wave function. The amount of the contribution of non-Kekulé structures should be an indication of the aromaticity of the systems.

Results and Discussion

The relative free energies at B3LYP/6-31+G(d,p) and G2 computational levels for the different azole configurations have been gathered in Table 1. Both methods provide similar results, the absolute minima for each salt being the same within the two computational methods. In addition, similar energy differences are obtained.

Among the configurations considered, the N2−σ one of the 1,2,3-triazole is not a minimum but a transition state of the interconversion process between the degenerate N1−σ and N3−σ minima. Surprisingly, the three derivatives of imidazole and pyrrole are more stable in their π configuration than in the N−σ one. These results have been confirmed by MP2/aug-cc-pVTZ calculation showing the same tendency. In the pentazolate derivatives, the difference between the N−σ and π structures decreases as the size of the alkaline atom increases, attaining similar stability in the case of potassium salts at the G2 computational level. For the remaining cases, where two nitrogen atoms are together in the azole, the N−σ configuration is clearly more stable and in several of the systems with sodium and potassium it is the unique minimum. However, the presence of additional nitrogen atoms attached to those bonded to the metal decreases the difference between the N−σ and π configurations, this effect being on average 5.8 kJ/mol for the lithium derivatives.

TABLE 2: Homolytic and Heterolytic Dissociation Enthalpy (kJ/mol) Calculated at the G2 Computational Level

azole	alkaline confign	homolytic dissociation			heterolytic dissociation		
		Li	Na	K	Li	Na	K
pyrrole	N−σ	303.7	255.4	265.4	605.5	519.2	463.7
pyrrole	π	349.6	281.6	302.8	651.4	545.4	501.1
pyrazole	N−σ	452.4	391.2	403.2	665.6	566.4	513.0
pyrazole	π	412.2			625.5		
imidazole	N−σ	337.5	278.9	291.7	593.7	497.0	444.4
imidazole	π	370.7	301.8	328.5	626.8	519.9	481.1
1,2,3-triazole	N1−σ	459.9	409.2	424.1	629.3	540.5	490.0
1,2,3-triazole	π	350.2	309.1	339.3	593.1	514.1	478.8
1,2,4-triazole	N1−σ	453.5	401.3	415.1	631.6	541.4	489.8
1,2,4-triazole	N4−σ	372.4	332.7	343.3	550.6	472.8	418.0
1,2,4-triazole	π	402.9			581.0		
tetrazole	N1−σ	478.2	437.0	454.5	588.4	509.2	461.2
tetrazole	N2−σ	478.6	439.0	457.3	588.8	511.2	464.0
tetrazole	π	441.5			551.7		
pentazole	N−σ	*a*			545.8	476.9	432.7
pentazole	π				517.3	460.3	435.3

[a] See the text for an explanation of the N_5 radical behavior.

In order to evaluate the bonding strength of the systems, the enthalpy of dissociation in a homolytic and a heterolytic process has been calculated (Table 2). In the case of the N_5 radical no stable cyclic structure has been obtained, in agreement with previous reports, since it tends to decompose into $N_2 + N_3$.[39–41] The most stable radicals obtained for the rest of the systems are similar to those previously described in the literature.[42–44]

The enthalpy of the homolytic dissociation is also known as bond dissociation energy (BDE). Since no experimental BDE is available for any of the systems studied here, we have calculated the NH BDE of the parent compounds of pyrrole, pyrazole and imidazole (401.4, 470.5 and 407.6 kJ/mol) for which experimental data are available (405.8,[45] 451.8[44] and 403.8[44]). The calculated results reproduce the experimental ones with acceptable differences.

The homolytic dissociation energies range between 255 and 478 kJ/mol; for comparative purposes the value of the BDE of the CC bond in ethane is 377.5 kJ/mol[45] and that of the lithium fluoride molecule in the gas phase 574.7 kJ/mol.[46] In general, the dissociation energy increases as the number of vicinal nitrogen atoms increases in the azole. Thus, the smallest dissociation energies correspond to the pyrrole derivatives and the largest ones to the tetrazole derivatives. It can be considered that the effective electronegativity of the heterocycle, as a whole, increases due to the presence of more nitrogen atoms. Regarding the effect of the alkaline metal in this magnitude, for a given configuration, always the weakest system corresponds to the sodium one, and in most of the cases the lithium derivative is more strongly bonded than the potassium one, but in a few cases the reverse is true.

The heterolytic dissociation, which corresponds to the formation of an anionic azolate and a cationic metallic atom, is larger than the corresponding heterolytic one. It ranges between 418 and 666 kJ/mol. In this case, the stronger complex, for a given

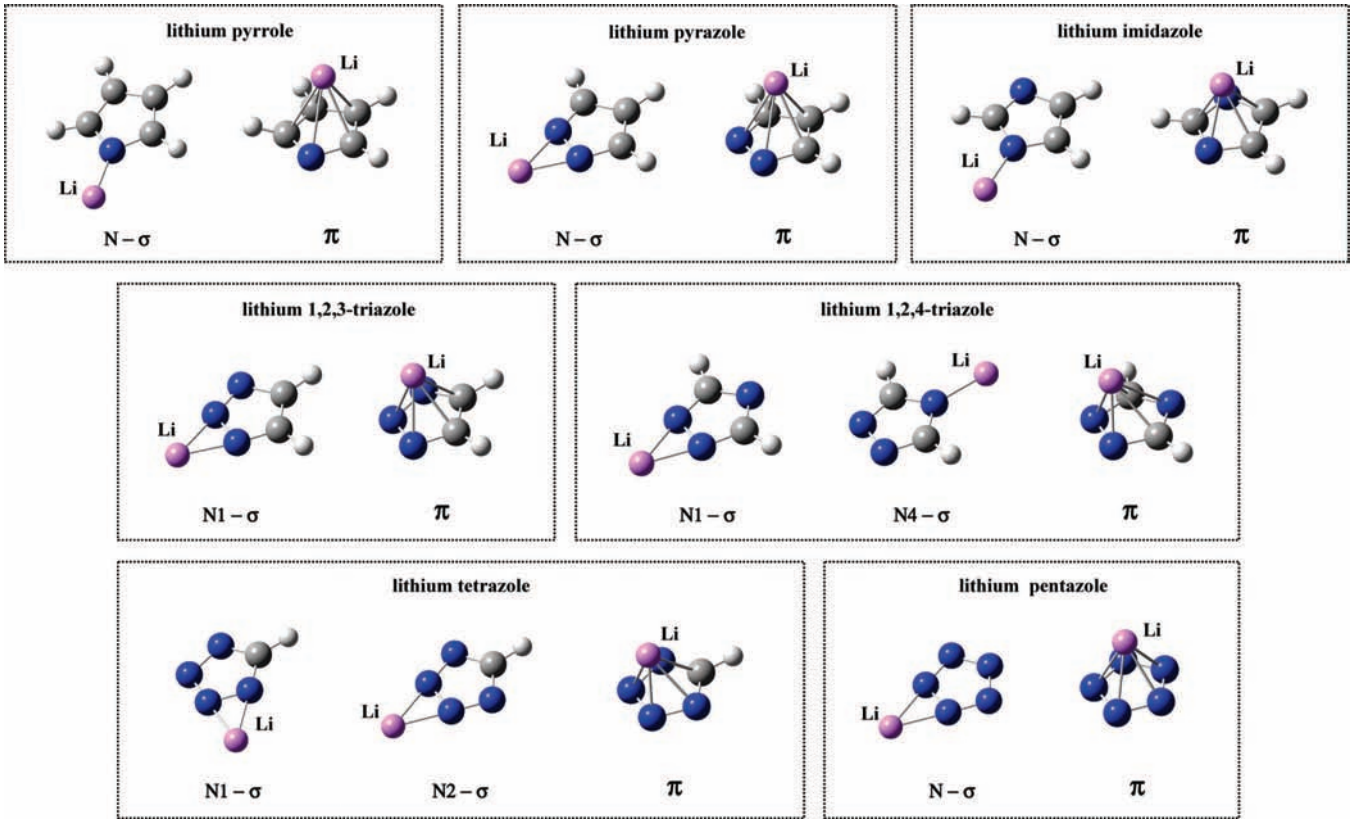

Figure 1. Optimized geometries of all the lithium derivatives considered.

configuration, corresponds to that formed with lithium, followed by the one with sodium, that of potassium being the weaker.

The distortion energy of the azole ring has been evaluated as the difference of the energy of the isolated azolate and that with the geometry within the alkaline derivatives. The values obtained show small distortion, the maximum being 4.2 kJ/mol. Some general tendencies observed are (i) the reduction of the distortion energy, for a given configuration, as the size of the alkaline atom increases; (ii) the σ configuration with the alkaline atom interacting with one nitrogen atom presents larger distortion energy than those where the interaction is with two nitrogen atoms and the corresponding π configuration presents the smallest distortion energies.

The optimized geometries of all the systems calculated for the lithium derivatives are shown in Figure 1 and gathered in Tables 3 and 4. The N$-\sigma$ configuration of these azoles having two contiguous nitrogen atoms shows the alkaline atoms interacting simultaneously with both nitrogens while, in all the cases that present a π structure, the alkaline atoms are at very similar distances of the five atoms of the ring, the largest differences in the distances to the ring atoms found for all the alkaline atoms being in the complex with the 1,2,3-triazole (0.36, 0.75 and 0.60 Å for the lithium, sodium and potassium derivative, respectively). In general, it can be stated that the bond distances of the alkaline atoms increase with the number of bonded atoms.

The structures of the azole derivatives have been compared to the corresponding isolated azolates (Table 4). In the case of the σ configuration, a lengthening of the bond N−N, when present, interacting with the alkaline metallic atom or, otherwise, the bond in α position to the one where the alkaline atom is attached can be observed, while a shortening is observed in those surrounding the previous bond. This effect is more important if the atoms involved in the bond are nitrogens, probably to the larger polarizability of the corresponding lone pairs of these atoms upon the bond formation with the alkaline atoms. In the cases studied, the maximum elongation observed is 0.026 Å for the N1−N2 bond of the 1-lithium-1,2,3-triazole and the maximum shortening is −0.028 Å for the N1−N2 bond for the 2-lithium-tetrazole.

For the complexes in π configuration, in general, all the bond distances are elongated this effect being smaller than those observed in the σ configuration. The maximum elongation obtained is 0.015 Å in the N2−N3 bond of the lithium-tetrazole, the average increment in all the bonds being 0.005 Å. These

TABLE 3: Nitrogen−Alkaline Atom Distance (Å) for the Systems in σ Configuration and Alkaline Atom−Center of the Ring Distance for Those in π Configuration

azole	alkaline confign	Li	Na	K
pyrrole	N$-\sigma$	1.804	2.144	2.523
pyrrole	π	1.747	2.220	2.648
pyrazole	N$-\sigma$	1.829	2.187	2.545
pyrazole	π	1.787		
imidazole	N$-\sigma$	1.812	2.154	2.536
imidazole	π	1.757	2.217	2.628
1,2,3-triazole	N1$-\sigma$	1.858/1.833[a]	2.228/2.185[a]	2.588/2.543[a]
1,2,3-triazole	π	1.809	2.380	2.703
1,2,4-triazole	N1$-\sigma$	1.844	2.201	2.561
1,2,4-triazole	N4$-\sigma$	1.819	2.161	2.549
1,2,4-triazole	π	1.829		
tetrazole	N1$-\sigma$	1.873/1.857[a]	2.242/2.202[a]	2.606/2.565[a]
tetrazole	N2$-\sigma$	1.865	2.225	2.587
tetrazole	π	1.830		
pentazole	N$-\sigma$	1.887	2.244	2.612
pentazole	π	1.830	2.24	2.621

[a] Indicate the distance to the nonsymmetrical N1 and N2, respectively.

TABLE 4: Bond Distances of the Azolate (Å) and Variation Observed in the Corresponding Alkaline Derivatives Calculated at the B3LYP/6-31+G(d,p) Computational Level

azole	alkaline atom	confign	X1−X2	X2−X3	X3−X4	X4−X5	X5−X1
pyrrolate			1.365	1.407	1.422	1.407	1.365
pyrrole	Li	N−σ	0.016	−0.019	0.001	−0.019	0.016
pyrrole	Na	N−σ	0.012	−0.015	−0.001	−0.015	0.012
pyrrole	K	N−σ	0.010	−0.012	−0.002	−0.012	0.010
pyrrole	Li	π	0.007	0.004	0.002	0.004	0.007
pyrrole	Na	π	0.007	0.003	0.003	0.003	0.007
pyrrole	K	π	0.007	0.001	0.001	0.001	0.004
pyrazolate			1.365	1.353	1.408	1.408	1.353
pyrazole	Li	N−σ	0.024	−0.010	−0.006	−0.006	−0.010
pyrazole	Na	N−σ	0.022	−0.007	−0.006	−0.006	−0.007
pyrazole	K	N−σ	0.019	−0.006	−0.006	−0.006	−0.006
pyrazole	Li	π	0.012	0.008	0.002	0.002	0.008
imidazolate			1.352	1.352	1.373	1.395	1.373
imidazole	Li	N−σ	0.018	−0.024	0.002	−0.015	0.014
imidazole	Na	N−σ	0.013	−0.020	0.000	−0.012	0.011
imidazole	K	N−σ	0.011	−0.016	−0.001	−0.010	0.010
imidazole	Li	π	0.007	0.007	0.003	0.007	0.003
imidazole	Na	π	0.005	0.005	0.004	0.005	0.004
imidazole	K	π	0.002	0.002	0.002	0.002	0.002
1,2,3-triazolate			1.344	1.344	1.357	1.393	1.357
1,2,3-triazole	Li	N−σ	0.026	−0.026	−0.004	0.001	−0.013
1,2,3-triazole	Na	N−σ	0.023	−0.021	−0.004	0.000	−0.009
1,2,3-triazole	K	N−σ	0.019	−0.017	−0.004	0.000	−0.008
1,2,3-triazole	Li	π	0.011	0.011	0.002	0.006	0.002
1,2,3-triazole	Na	π	0.008	0.008	−0.001	0.003	−0.001
1,2,3-triazole	K	π	0.004	0.004	0.000	0.003	0.000
1,2,4-triazolate			1.378	1.339	1.356	1.356	1.339
1,2,4-triazole	Li	N1−σ	0.019	−0.005	−0.010	−0.010	−0.005
1,2,4-triazole	Li	N4−σ	0.000	−0.019	0.016	0.016	−0.019
1,2,4-triazole	Na	N1−σ	0.019	−0.004	−0.009	−0.009	−0.004
1,2,4-triazole	Na	N4−σ	0.001	−0.016	0.013	0.013	−0.016
1,2,4-triazole	K	N1−σ	0.016	−0.003	−0.008	−0.008	−0.003
1,2,4-triazole	K	N4−σ	−0.001	−0.013	0.011	0.011	−0.013
1,2,4-triazole	Li	π	0.008	0.010	0.001	0.001	0.010
tetrazolate			1.352	1.324	1.352	1.341	1.341
tetrazole	Li	N1−σ	0.019	−0.016	−0.012	−0.002	−0.006
tetrazole	Li	N2−σ	−0.028	0.024	−0.028	0.003	0.003
tetrazole	Na	N1−σ	0.018	−0.013	−0.011	−0.002	−0.004
tetrazole	Na	N2−σ	−0.024	0.023	−0.024	0.002	0.002
tetrazole	K	N1−σ	0.013	−0.010	−0.010	−0.002	−0.003
tetrazole	K	N2−σ	−0.019	0.018	−0.019	0.001	0.001
tetrazole	Li	π	0.002	0.015	0.002	0.006	0.006
pentazolate			1.329	1.329	1.329	1.329	1.329
pentazole	Li	N−σ	0.016	−0.016	−0.002	−0.002	−0.016
pentazole	Na	N−σ	0.017	−0.014	−0.002	−0.002	−0.014
pentazole	K	N−σ	0.013	−0.011	−0.002	−0.002	−0.011
pentazole	Li	π	0.007	0.007	0.007	0.007	0.007
pentazole	Na	π	0.004	0.004	0.004	0.004	0.004
pentazole	K	π	0.002	0.002	0.002	0.002	0.002

effects, both in σ and in π complexes, decrease in magnitude as the size of the alkaline metal increases.

The main differences in the geometries observed for the molecules in N−σ and π configurations can be associated with the presence of an alkaline atom linked to a nitrogen atom in the first case that is replaced in the second by an isolated lone pair. Thus, in the NBO analysis the interaction between the nitrogen lone pair and the antibonding orbital in β position is larger for the systems in π configuration than in the N−σ ones. For instance in the case of the lithiumpyrrole in the π configuration, the orbital interaction between the lone pair of the N1 with the C2−C3 (or C4−C5) antibonding orbital amounts to 64.32 kcal/mol while in the N−σ it is only 43.06 kcal/mol. This interaction is associated with a charge transfer from the occupied orbital to the antibonding one which produces an elongation of the bond of the latter orbital. This effect is larger in the lithium molecules than in the sodium or potassium ones, the different in the bond distances being up to 0.03 Å. Similar results have been described for other systems.[47,48]

The charges calculated with the NBO methods (Table 5) show values in the alkaline atoms close to 1 being smaller for the π configuration than those of the corresponding N−σ one. The total bond order, obtained with the NBO method, of the alkaline atoms is closely related to the charge. Those alkaline atoms with larger charge present lower bond orders. For a given alkaline atom, the larger differences of charge between the π and N−σ configurations correspond to the pyrrole and imidazole systems. The smaller charges for a given alkaline atom always correspond to the π configuration of the pyrrole and the largest to the N4−σ of the 1,2,4-triazole. For each given system, as the alkaline atom increases, the charge in the metal increases.

Due to the unexpected and interesting behavior of the pyrrole and imidazole anions, where the π configuration is the most stable one, we have focused the rest of our study on those derivatives.

The topological analysis of the electron density shows the presence of a unique bond critical point (bcp) in the N−σ complexes of pyrrole and imidazole while several bcp are found

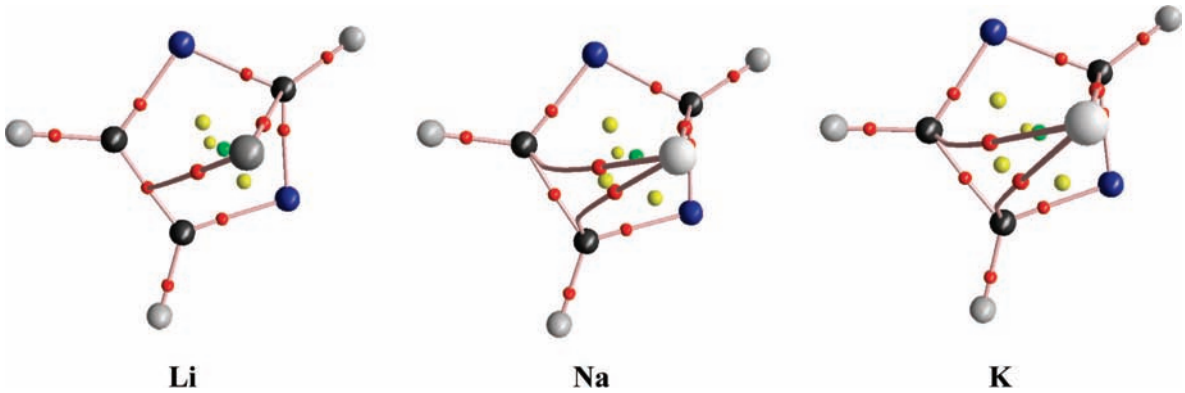

Figure 2. Molecular graph of the imidazolate derivatives in π configuration. Red, yellow and green balls indicate the bond, ring and cage critical points.

TABLE 5: Calculated Charges (e) on the Metal Atoms with the NBO Method at the B3LYP/6-31+G(d,p) Computational Level

azole	alkaline confign	Li	Na	K
pyrrole	N−σ	0.920	0.927	0.960
pyrrole	μ	**0.770**	**0.884**	**0.934**
pyrazole	N−σ	0.850	0.913	0.954
pyrazole	μ	0.802		
imidazole	N−σ	0.927	0.930	0.961
imidazole	μ	0.800	0.902	0.942
1,2,3-triazole	N1−σ	0.863	0.915	0.955
1,2,3-triazole	μ	0.822	0.919	0.943
1,2,4-triazole	N1−σ	0.869	0.920	0.957
1,2,4-triazole	N4−σ	**0.932**	**0.937**	**0.966**
1,2,4-triazole	μ	0.836		
tetrazole	N1−σ	0.880	0.925	0.960
tetrazole	N2−σ	0.872	0.919	0.957
tetrazole	μ	0.844		
pentazole	N−σ	0.890	0.931	0.963
pentazole	μ	0.853	0.922	0.945

TABLE 6: Integrated Properties of the Azole Ring Moiety and Total Volume (a.u.) within the AIM Methodology

azole	alkaline atom	confign	energy	charge	volume	total molecular volume
pyrrole	Li	N−σ	−209.74946	−0.928	693.5	722.0
pyrrole	Li	μ	−209.75619	−0.893	685.1	714.5
pyrrole	Na	N−σ	−209.30849	−0.896	693.7	766.7
pyrrole	Na	μ	−209.27408	−0.907	688.3	757.7
pyrrole	K	N−σ	−208.40130	−0.914	695.2	848.6
pyrrole	K	μ	−208.43577	−0.897	681.6	832.4
imidazole	Li	N−σ	−225.80769	−0.932	650.6	679.1
imidazole	Li	μ	−225.81681	−0.903	639.4	668.3
imidazole	Na	N−σ	−225.40463	−0.897	649.9	723.0
imidazole	Na	μ	−225.35738	−0.920	643.0	706.3
imidazole	K	N−σ	−224.44082	−0.918	650.5	803.5
imidazole	K	μ	−224.48527	−0.909	638.7	788.8

between the metal and the atoms of the heterocycles in the π configuration. In addition, and depending on the nature of the alkaline atoms, the topological description changes as shown in Figure 2 for the imidazole derivates. While the lithium salt presents a T shape interaction with the C3C4 atoms, in the sodium and potassium derivatives, it turns out to be a V shape. In addition the V becomes wider for the latter case.

The integrated properties within the atomic basins using the atom in molecules (AIM) methodology (Table 6) show that the azole ring is more stable in the π configuration for the lithium and potassium derivatives and in the N−σ one for the sodium cases. The value of the charges parallels these results being more negative for the more stable rings. Thus, the charge results obtained for the sodium with the AIM method are opposite to the ones obtained for the NBO one, while the rest of the cases follow the same tendency. Regarding the volume calculated using a 0.001 au electronic isosurface of the azole moiety and the total molecule, in both cases the systems in π configuration present a smaller volume than their counterpart in N−σ configuration. These results indicate that, under high pressure conditions, the π configuration will be over stabilized vs the N−σ one.

The analysis of the molecular electrostatic potential (MEP) of the salts shows that the N−σ systems present negative regions above and below the heterocyclic rings that mostly disappear in the π cases, in favor of a negative region in the nitrogen atoms that previously was bonded to the alkaline metal (Figure 3). The values of the MEP minima have been gathered in Table 7. An increment of the MEP value is observed, for each family of compounds, as the size of the alkaline atom increases, in agreement with the charge variation in the metal previously mentioned for the NBO method. A linear correlation can be found between the value of the MEP minima and the distances listed in Table 5. A similar tendency has been recently described for a large series of β and γ derivatives of pyridine.[49] It should be noted that the location and value of the MEP minima has been associated with the protonation,[49] hydrogen bond formation and electrophilic attacks. Thus, the importance of the changes has been observed.

The aromaticity of these derivatives has been evaluated by means of the NICS(1) and HOMA (Table 8). For comparative purposes, those of the anions and for the parent compounds have been included. Based on the NICS(1), the alkaline derivatives are more aromatic than the parent compound and

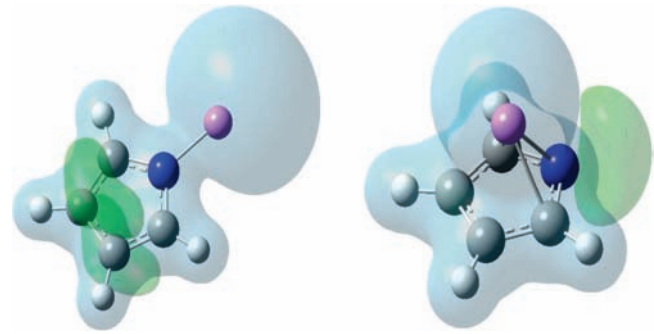

Figure 3. Electrostatic potential of the two lithium derivatives of pyrrole.

TABLE 7: Value of the MEP Minima (a.u.) and Distance (Å) to the Nitrogen Atom or to the Plane of the Azole

azole	alkaline atom	config	MEP	distance to N	distance to the ring
pyrrole	Li	N−σ	−0.065		1.603
pyrrole	Na	N−σ	−0.077		1.579
pyrrole	K	N−σ	−0.089		1.560
pyrrole	Li	μ	−0.117	1.277	
pyrrole	Na	μ	−0.132	1.266	
pyrrole	K	μ	−0.143	1.258	
imidazole	Li	N−σ	−0.133	1.268	
imidazole	Na	N−σ	−0.154	1.264	
imidazole	K	N−σ	−0.165	1.258	
imidazole	Li	μ	−0.105	1.288	
imidazole	Na	μ	−0.121	1.275	
imidazole	K	μ	−0.133	1.266	

TABLE 8: NICS(1) (ppm) and HOMA Aromaticity Indexes of the Pyrrole and Imidazole Derivatives

		pyrrole		imidazole	
derivative	config	NICS(1)	HOMA	NICS(1)	HOMA
anion		−10.26	0.868	−10.88	0.928
H	N−σ	−10.09[a]	0.849[a]	−10.58[b]	0.884[b]
Li	N−σ	−10.34	0.853	−11.00	0.887
Li	μ	−11.18	0.821	−11.64	0.899
Na	N−σ	−10.30	0.871	−11.01	0.905
Na	μ	−10.33	0.825	−10.91	0.903
K	N−σ	−10.38	0.879	−11.11	0.912
K	μ	−10.95	0.848	−11.47	0.916

[a] Values taken from ref 50. [b] Values taken from ref 51.

the corresponding anion, the π configuration being slightly more aromatic than the σ counterpart. The results of the HOMA index are more complex, and the only clear tendency is the increment of the aromaticity as the metal size increases for a given azole and configuration.

Natural resonance theory furnishes the weight of each of the contributing Lewis structures to the *ab initio* wave function. For the parent azoles, the single principal, or Kekulé, structure accounts between 50 and 70%.[52] The participation of the non-Kekulé forms should be related to the aromaticity of these systems. In the molecules considered here, the values of the Kekulé forms vary between 23 and 15%, and thus, this partition indicates that they are more aromatic than the parent compounds. The π configuration is more aromatic, based on this analysis, but the difference with the N−σ one decreases as the size of the alkaline atom increases.

A CSD search[53] of neutral alkaline salts of the system with pyrrole and imidazole moieties, those with stable π configurations, has yielded 36 structures that present the alkaline atom above the heterocyclic system similar to those proposed in the present communication (Table 9). The distances observed experimentally depend on the size of the metal atoms. Thus, the lithium derivatives present distances between 1.83 and 2.18, sodium 2.38 and 2.72 and potassium 2.78 and 3.10 Å. In general, the angles are close to 90°, which indicates that the mentioned atoms are above the heterocyclic rings. The observed experimental distances are longer than those reported in the theoretical calculations, but the surrounding atoms in the crystal structure have important influence in the measured distances while in the calculation the system are completely isolated.

TABLE 9: CSD Refcodes of the Structures That Present an Alkaline Pyrrolate or Imidazolate in π Configuration

refcode	azole moiety	alkaline atom	distance	angle[a]
AHISOZ	pyrrole	K	2.827[b]	85.9
BAQVAQ	pyrrole	Na	2.502	84.9
BAQVEU	pyrrole	Na	2.718	114.0
HOTKIK - r1	pyrrole	Li	1.904	86.5
HOTKIK - r2	pyrrole	Li	2.184	92.9
ILISUR - r1	pyrrole	K	2.921	85.8
ILISUR - r1	pyrrole	K	3.103	94.7
ILITEC	pyrrole	Li	1.972	88.4
KICFIL	pyrrole	Na	2.378	91.5
PERWEO	pyrrole	K	2.878	86.7
QACWIA - r1	pyrrole	Li	2.076	84.0
QACWIA - r2	pyrrole	Li	2.093	86.6
RISREQ	pyrrole	K	2.845	88.0
XALRIM	pyrrole	K	2.954	87.4
XALROS - r1	pyrrole	K	2.876	77.6
XALROS - r2	pyrrole	K	2.911	77.0
XARQUEN - r1	pyrrole	K	2.891	91.9
XARQUEN - r2	pyrrole	K	2.935	87.3
XARQUEN - r3	pyrrole	K	2.816	84.6
XEMHUS - r1	pyrrole	K	2.792	93.3
XEMHUS - r2	pyrrole	K	2.910	85.0
XEMHUS - r3	pyrrole	K	2.972	85.0
XEMHUS - r4	pyrrole	K	2.859	93.6
XEMHUS - r5	pyrrole	K	2.823	81.0
XEMHUS - r6	pyrrole	K	2.781	84.2
ZALCOE - r1	pyrrole	Li	1.829	90.7
ZALCOE - r2	pyrrole	Li	1.848	89.2
YAKWUD	pyrrole	Rb	3.010	77.8
XEMHOM	pyrrole	Cs	3.069	88.2
YAKXAK	pyrrole	Cs	3.534	65.4
YAKXAK	pyrrole	Cs	3.134	84.1
UCUJOR	imidazole	Cs	3.099	89.6
UCUJOR	imidazole	Cs	3.151	83.9
UCUJOR	imidazole	Cs	3.099	90.2
UCUJUX	imidazole	Cs	3.293	82.5
UCUJUX	imidazole	Cs	3.293	97.2

[a] Angle defined as metal−center of the ring-N1. [b] Taken from ref 54 since no coordinates were available in the CSD database.

Conclusions

A theoretical study of the alkaline metal derivative of azoles has been carried out by means of B3LYP/6-31+G(d,p) and G2 calculations. The results show that the pyrrole and imidazole derivatives prefer the disposition with the metal atom in π configuration while, in the rest of the cases, the N−σ one is more stable. We have found in the CSD database several structures of alkaline pyrrole and imidazole systems in π configuration. These π structures must be considered when discussing the chemical and biological properties of azoles.

Since for the potassium pentazolate salt[39,55–57] both configurations have similar energies (G2 calculations), this molecule should be a promising structure to be studied experimentally.

A comparison of the electronic properties of these two configurations has been carried out by studying their molecular electrostatic potential and the properties derived from the electron density. Significant differences are found in these properties between the N−σ and π configurations which can affect the surrounding environment.

Acknowledgment. This work was carried out with financial support from the Ministerio de Educación y Ciencia (Project No. CTQ2007-61901/BQU) and Comunidad Autónoma de Madrid (Project MADRISOLAR, ref S-0505/PPQ/0225). Thanks are given to the CTI (CSIC) and CESGA for allocation of computer time. We would like to thank an anonymous referee for helpful comments on this article.

Supporting Information Available: Optimized geometry of all the systems studied at the B3LYP/6-31+G(d,p) computational level. This material is available free of charge via the Internet at http://pubs.acs.org.

References and Notes

(1) Meyer, E. A.; Castellano, R. K.; Diederich, F. *Angew. Chem., Int. Ed.* **2003**, *42*, 1210.

(2) Banerjee, R.; Phan, A.; Wang, B.; Knobler, C.; Furukawa, H.; O'Keeffe, M.; Yaghi, O. M. *Science* **2008**, *319*, 939.

(3) Headley, A. D.; Ni, B. *Aldrichimica Acta* **2007**, *40*, 107.

(4) Elguero, J. In *Comprehensive Heterocyclic Chemistry II*; Pergamon-Elsevier: Oxford, 1996; Vol. 3; pp 1.

(5) Katritzky, A. R.; Singh, S.; Kirichenko, K.; Smiglak, M.; Holbrey, J. D.; Reichert, W. M.; Spear, S. K.; Rogers, R. D. *Chem. Eur. J.* **2006**, *12*, 4630.

(6) Sygula, A.; Rabideau, P. W. *J. Am. Chem. Soc.* **1992**, *114*, 821.

(7) Cortes-Llamas, S.; Velazquez-Carmona, M. A.; Munoz-Hernandez, M. A. *Inorg. Chem. Commun.* **2005**, *8*, 155.

(8) Cortes-Llamas, S. A.; Hernandez-Lamoneda, R.; Velazquez-Carmona, M. A.; Munoz-Hernandez, M. A.; Toscano, R. A. *Inorg. Chem.* **2006**, *45*, 286.

(9) Beaini, S.; Deacon, G. B.; Erven, A. P.; Junk, P. C.; Turner, D. R. *Chem. Asian J.* **2007**, *2*, 539.

(10) Heldt, I.; Behrens, U. *Z. Anorg. Allg. Chem.* **2005**, *631*, 749.

(11) Zhao, J. F.; Li, N.; Li, Q. S. *Theor. Chim. Acta* **2003**, *110*, 10.

(12) Becke, A. D. *J. Chem. Phys.* **1993**, *98*, 5648.

(13) Lee, C. T.; Yang, W. T.; Parr, R. G. *Phys Rev B* **1988**, *37*, 785.

(14) Hariharan, P. C.; Pople, J. A. *Theor. Chim. Acta* **1973**, *28*, 213.

(15) Frisch, M. J. ; Trucks, G. W.; Schlegel, H. B.; Scuseria, G. E.; Robb, M. A.; Cheeseman, J. R.; Montgomery, J., J. A.; Vreven, T.; Kudin, K. N.; Burant, J. C.; Millam, J. M.; Iyengar, S. S.; Tomasi, J.; Barone, V.; Mennucci, B.; Cossi, M.; Scalmani, G.; Rega, N.; Petersson, G. A.; Nakatsuji, H.; Hada, M.; Ehara, M.; Toyota, K.; Fukuda, R.; Hasegawa, J.; Ishida, M.; Nakajima, T.; Honda, Y.; Kitao, O.; Nakai, H.; Klene, M.; Li, X.; Knox, J. E.; Hratchian, H. P.; Cross, J. B.; Bakken, V.; Adamo, C.; Jaramillo, J.; Gomperts, R.; Stratmann, R. E.; Yazyev, O.; Austin, A. J.; Cammi, R.; Pomelli, C.; Ochterski, J. W.; Ayala, P. Y.; Morokuma, K.; Voth, G. A.; Salvador, P.; Dannenberg, J. J.; Zakrzewski, V. G.; Dapprich, S.; Daniels, A. D.; Strain, M. C.; Farkas, O.; Malick, D. K.; Rabuck, A. D.; Raghavachari, K.; Foresman, J. B.; Ortiz, J. V.; Cui, Q.; Baboul, A. G.; Clifford, S.; Cioslowski, J.; Stefanov, B. B.; Liu, G.; Liashenko, A.; Piskorz, P.; Komaromi, I.; Martin, R. L.; Fox, D. J.; Keith, T.; Al-Laham, M. A.; Peng, C. Y.; Nanayakkara, A.; Challacombe, M.; Gill, P. M. W.; Johnson, B.; Chen, W.; Wong, M. W.; Gonzalez, C.; Pople, J. A. *Gaussian-03*; Gaussian, Inc.: Wallingford, CT, 2003.

(16) Curtiss, L. A.; Carpenter, J. E.; Raghavachari, K.; Pople, J. A. *J. Chem. Phys.* **1992**, *96*, 9030.

(17) Møller, C.; Plesset, M. S. *Phys. Rev.* **1934**, *46*, 618.

(18) Dunning, T. H. *J. Chem. Phys.* **1989**, *90*, 1007.

(19) Bader, R. F. W. *Atoms in Molecules: A Quantum Theory*; Clarendon Press: Oxford, 1990.

(20) Biegler-König, F. W.; Bader, R. F. W.; Tang, T. H. *J. Comput. Chem.* **1982**, *3*, 317.

(21) Popelier, P. L. A., with a contribution from R. G. A. Bone (UMIST, Engl, EU) MORPHY98, a topological analysis program; 0.2 ed., 1999.

(22) Biegler-König, F. W.; Schönbohm, J. *AIM2000*, 2.0 ed.; Bielefeld, Germany, 2002.

(23) Alkorta, I.; Picazo, O. *Arkivoc* **2005**, *ix*, 305.

(24) Weinhold, F.; Landis, C. R. *Valency and Bonding. A Natural Bond Orbital Donor-Aceptor Perspective*; Cambridge Press: Cambridge, 2005.

(25) Glendening, E. D.; Reed, A. E.; Carpenter, J. E.; Weinhold, F. *NBO*, version 3.1.

(26) Glendening, E. D.; J, K. B.; Reed, A. E.; Carpenter, J. E.; Bohmann, J. A.; Morales, C. M.; Weinhold, F. *NBO 5.0*; Theoretical Chemistry Institute, University of Wisconsin: Madison, 2001.

(27) Politzer, P.; Truhlar, D. G. *Chemical Applications of atomic and molecular electrostatic Potentials*; Plenum Press: New York, 1981.

(28) Alkorta, I.; Villar, H. O.; Arteca, G. A. *J. Comput. Chem.* **1993**, *14*, 530.

(29) Solimannejad, M.; Alkorta, I.; Elguero, J. *J Phys Chem A* **2007**, *111*, 2077.

(30) Alkorta, I.; Bachs, M.; Perez, J. J. *Chem. Phys. Lett.* **1994**, *224*, 160.

(31) Alkorta, I.; Villar, H. O.; Perez, J. J. *J. Phys. Chem.* **1993**, *97*, 9113.

(32) Murray, J. S.; Ken, K. *Molecular Electrostatic Potentials*; Elsevier: New York, 1996.

(33) Krygowski, T. M. *J. Chem. Inf. Comput. Sci.* **1993**, *33*, 70.

(34) Schleyer, P. v. R.; Maerker, C.; Dransfeld, A.; Jiao, H. J.; Hommes, N. J. R. V. *J. Am. Chem. Soc.* **1996**, *118*, 6317.

(35) Schleyer, P. v. R.; Manoharan, M.; Wang, Z. X.; Kiran, B.; Jiao, H. J.; Puchta, R.; Hommes, N. J. R. V. *Org. Lett.* **2001**, *3*, 2465.

(36) Glendening, E. D.; Weinhold, F. *J. Comput. Chem.* **1998**, *19*, 593.

(37) Glendening, E. D.; Weinhold, F. *J. Comput. Chem.* **1998**, *19*, 610.

(38) Glendening, E. D.; Badenhoop, J. K.; Weinhold, F. *J. Comput. Chem.* **1998**, *19*, 628.

(39) Nguyen, M. T.; Ha, T.-K. *Chem. Phys. Lett.* **2001**, *335*, 311.

(40) Nguyen, M. T.; Ha, T.-K. *Chem. Phys. Lett.* **2000**, *317*, 135.

(41) Nguyen, M. T. *Coord. Chem. Rev.* **2003**, *244*, 93.

(42) Gianola, A. J.; Ichino, T.; Kato, S.; Bierbaum, V. M.; Lineberger, W. C. *J. Phys. Chem. A* **2006**, *110*, 8457.

(43) Alkorta, I.; Elguero, J. *Tetrahedron* **2006**, *62*, 8683.

(44) daSilva, G.; Moore, E. E.; Bozzelli, J. W. *J. Phys. Chem. A* **2006**, *110*, 13979.

(45) Luo, Y. R. *Handbook of bond dissociation energies in organic compounds*; CRC Press: Boca Raton, 2003.

(46) Brewer, L.; Brackett, E. *Chem. Rev.* **1961**, *61*, 425.

(47) Abboud, J. L. M.; Koppel, I. A.; Alkorta, I.; Della, E. W.; Muller, P.; Davalos, J. Z.; Burk, P.; Koppel, I.; Pihl, V.; Quintanilla, E. *Angew. Chem., Int. Ed.* **2003**, *42*, 2281.

(48) Abboud, J. L. M.; Alkorta, L.; Burk, P.; Davalos, J. Z.; Quintanilla, E.; Della, E. W.; Koppel, I. A.; Koppel, I. *Chem. Phys. Lett.* **2004**, *398*, 560.

(49) Blanco, F.; O'Donovan, D. H.; Alkorta, I.; Elguero, J. *Struct. Chem.* **2008**, *19*, 339.

(50) Zborowski, K.; Alkorta, I.; Elguero, J. *Struct. Chem.* **2007**, *18*, 797.

(51) Blanco, F.; Alkorta, I.; Zborowski, K.; Elguero, J. *Struct. Chem.* **2007**, *18*, 965.

(52) Bean, G. P. *J. Org. Chem.* **1998**, *63*, 2497.

(53) Allen, F. H.; Davies, J. E.; Galloy, J. J.; Johnson, O.; Kennard, O.; Macrae, C. F.; Mitchell, E. M.; Mitchell, G. F.; Smith, J. M.; Watson, D. G. *J. Chem. Inf. Comput. Sci.* **1991**, *31*, 187.

(54) Evans, W. J.; Brady, J. C.; Ziller, J. W. *Inorg. Chem.* **2002**, *41*, 3340.

(55) Nguyen, M. T.; McGinn, M. A.; Hegarty, A. F.; Elguero, J. *Polyhedron* **1985**, *4*, 1721.

(56) Nguyen, M. T.; Sana, M.; Leroy, G.; Elguero, J. *Can. J. Chem.* **1983**, *61*, 1435.

(57) Butler, R. N.; Hanniffy, J. M.; Stephens, J. C.; Burke, L. A. *J. Org. Chem.* **2008**, *73*, 1354.

JP801936V